Vol. 129: 31–39, 2018
https://doi.org/10.3354/dao03234

DISEASES OF AQUATIC ORGANISMS
Dis Aquat Org

Published June 19

Histopathological, ultrastructural and molecular phylogenetic analysis of a novel microsporidium in a loggerhead sea turtle *Caretta caretta*

S. A. Martinson[1,*], S. J. Greenwood[2], D. Wadowska[1], K. Martin[3]

[1]Department of Pathology and Microbiology, Atlantic Veterinary College, University of Prince Edward Island, 550 University Avenue, Charlottetown, PE C1A 4P3, Canada

[2]Department of Biomedical Science, Atlantic Veterinary College, University of Prince Edward Island, 550 University Avenue, Charlottetown, PE C1A 4P3, Canada

[3]Canadian Sea Turtle Network, 6156 Quinpool Road, Suite 101, Halifax, NS B3L 1A3, Canada

ABSTRACT: Microsporidial spores were identified in the musculature of a loggerhead sea turtle *Caretta caretta* found dead on the shore in New Brunswick, Canada. Gastroenteritis was diagnosed on gross postmortem examination, with no gross abnormalities detected in the skeletal muscle. Histologically, the microsporidial spores were associated with inflammation and muscular necrosis and measured 1.1–1.7 × 2.2–3.4 µm. Spores were typically identified within sporophorous vesicles and, less often, in sporophorocysts and were weakly Gram positive, had punctate PAS staining, and were occasionally strongly acid-fast. Ultrastructural characteristics included 7–10 polar filament coils and other standard features of microsporidial spores. PCR for the microsporidial small subunit rRNA gene sequence was performed on DNA extracted from the muscle and small intestine, and the resulting amplicon was sequenced and queried against published microsporidial genomes. DNA sequences shared 98.2–99.8% sequence identity to Clade III of the Marinosporidia. This is the first report of a microsporidial infection contributing to the mortality of a sea turtle.

KEY WORDS: Microsporidium · Small subunit rRNA · SSU rRNA · *Caretta caretta* · Muscle · Reptile

INTRODUCTION

Loggerhead sea turtles *Caretta caretta* are distributed widely and can be found in the Atlantic, Pacific and Indian oceans (Bolten et al. 2011). Based on geographical location, they are split into 10 subpopulations, with loggerhead sea turtles in Atlantic Canada consisting of juveniles belonging to the Northwest Atlantic distinct population segment (DPS) (DFO 2017). While the Northwest Atlantic DPS is currently listed as a species of least concern by the IUCN, the global population of loggerhead sea turtles is currently listed as Vulnerable on the IUCN Red List of Threatened Species (Casale & Tucker 2015).

Threats to this species are primarily anthropogenic and include bycatch in fisheries, entanglement in fishing gear, traumatic injury from boat strike, noise and light pollution, marine contaminants, ingestion of plastic debris, illegal and legal harvest, and beach and coastal development; non-anthropogenic threats include predation and infectious disease (Bolten et al. 2011, DFO 2017). While anthropogenic causes of mortality in sea turtles are well described, there is a paucity of information regarding infectious disease in these species, warranting further research in this area (Galois & Ouelett 2007, Bolten et al. 2011).

Microsporidia are obligate intracellular eukaryotic pathogens that comprise a group of over 1500 species (Stentiford et al. 2013b). Previously considered protozoa, these unicellular organisms have been compared to fungi and, more recently, have been proposed to be closely related to the Cryptomycota (James et al.

*Corresponding author: smartinson@upei.ca

2013). Microsporidia have a wide host range, infecting every phyla of animal including both invertebrate and vertebrate species (Stentiford et al. 2013b), and reports of these infections appear to be increasing in frequency in reptiles. Among the 4 major groups of reptiles, microsporidial infections are most commonly reported in the Squamata (lizards and snakes) (Narasimhamurti et al. 1982, Jacobson et al. 1998, Koudela et al. 1998, Garner et al. 2000, Mitchell & Garner 2011, Richter et al. 2013, 2014, Gillett et al. 2016, Sokolova et al. 2016), with a single report of microsporidiosis occurring in each of the Rhynchocephalia (tuataras) (Liu & King 1971), the Crocodilia (crocodiles and alligators) (Scheelings et al. 2015) and the Testudines (turtles and tortoises) (Eydner et al. 2017). Among these reports, infections were typically found in captive reptiles, with rare reports in free-ranging animals (Narasimhamurti et al. 1982, Gillett et al. 2016). In the absence of monitoring programs for microsporidiosis in wild reptiles, however, it is difficult to comment on the prevalence of these infections in wild species (Stentiford et al. 2016).

Microsporidial infections have not been reported in any wild reptile species in Canada (Galois & Ouelett 2007) nor in any species of marine turtle to date. This study describes a microsporidial infection as a contributing factor in the death of a loggerhead sea turtle found on the shoreline in Atlantic Canada. The histopathological characteristics, ultrastructural features and molecular phylogenetic analysis of a partial small subunit rRNA (SSU rRNA) sequence of this novel microsporidial species are described.

MATERIALS AND METHODS

History and gross examination

A female juvenile loggerhead sea turtle measuring 49 cm in curved carapace length and 48.5 cm in curved carapace width was found dead on a beach, near the high-tide mark, in Cap-Lumière, New Brunswick (46.6596° N, 64.7092° W) on December 5, 2016. The frozen carcass was submitted by the Canadian Sea Turtle Network to the Canadian Wildlife Health Cooperative at the Atlantic Veterinary College, University of Prince Edward Island, for postmortem examination. The animal weighed 13.8 kg and was deemed to be in good body condition with moderate adipose stores and normal muscle mass. Gross abnormalities were largely restricted to the alimentary tract. Brown to pink-tinged fluid was present in the stomach, and there were small (1–2 mm) raised white plaques on the gastric mucosal surface. A fibrin cast was present in the lumen of the proximal small intestine, and the mucosa had yellow discolouration. The large intestinal content was abundant, brown and watery, with well-formed feces present distally. Routine aerobic bacteriologic culture of the small intestinal content yielded scant growth of *Serratia liquefaciens*.

Histopathology

Tissues collected during necropsy were fixed in 10% neutral buffered formalin, processed routinely, embedded in paraffin, sectioned at 5 µm thickness, and stained with hematoxylin and eosin. Slides, including samples of skeletal muscle, brain, heart, lung, liver, kidney, ovary, adrenal gland, stomach, small intestine and colon, were evaluated by a pathologist via light microscopy. In addition, periodic acid-Schiff (PAS) reaction, Ziehl-Neelsen (ZN) acid-fast and Gram stains were applied to the slides of skeletal muscle, small intestine, and stomach.

Transmission electron microscopy

Sections of formalin-fixed skeletal muscle were fixed overnight at 4°C in 2% buffered glutaraldehyde and postfixed in buffered 1% osmium tetroxide for 1 h at room temperature. Following fixation, the tissue was dehydrated in ascending concentrations of ethanol, cleared in propylene oxide, and infiltrated with a mixture of propylene oxide and epon resin. Tissue immersed in 100% epon was left in a vacuum overnight. Cubes of tissue were placed in BEEM capsules and polymerized in the oven at 70°C overnight. Thick and thin sections were cut on a Reicher Jung ultramicrotome. Thick sections were stained with 1% toluidine blue, and thin sections were stained with 5% uranyl acetate followed by Sato's lead stain. Sections were viewed on a Hitachi 7500 electron microscope at 80 kV. Digital images were taken with an AMT HR 40 camera.

DNA extraction, PCR and sequencing

DNA was extracted separately from four ~20 mg pieces of fresh-frozen skeletal muscle tissue and small intestine using a DNeasy blood and tissue kit (Qiagen) as per the manufacturer's instructions, except that the proteinase K digestion was for 2.5 to

22 h. PCR specific for the SSU rRNA gene sequence (~1300 bp partial sequence) was performed using universal microsporidial-specific primers 18f (5′-CAC CAG GTT GAT TCT GCC-3′) and 1492r (5′-GGT TAC CTT GTT ACG ACT T-3′) (Ghosh & Weiss 2009). Each PCR reaction was performed in a 25 µl reaction volume, comprising 6 µl (140–240 ng) of DNA, 2.5 µl of 10X PCR buffer (Qiagen), 0.5 µl of dNTP at 1.25 mM (Qiagen), 2.5 µl each of 18f and 1492r primer (10 µM), 1.25 units of HotStarTaq (Qiagen) and the remaining volume made of nuclease-free water. Negative control samples with 6 µl of nuclease-free water were conducted in place of DNA. PCR followed a touchdown protocol with an initial denaturation/activation step at 95°C for 2 min, followed by 30 cycles of 94°C for 1 min, 60°C for 45 s (decreasing by 0.5°C each cycle to 50°C for 45 s), 72°C for 2 min and a final extension at 72°C for 10 min. PCR amplicons were visualized after 1% agarose gel electrophoresis with SYBR Safe DNA gel stain (Thermo Fisher Scientific) under an ultraviolet light source.

DNA sequencing and phylogeny reconstruction

PCR amplicons of the expected size were sequenced in both directions using primers 18f, 1492R, 530f (5′-GTG CCA GC(C/A) GCC GCG G-3′) and 530r (5′-CCG CGG (T/G)GC TGG CAC-3′) (Vossbrinck et al. 2004, Ghosh & Weiss 2009) at the McGill University (Montreal, Canada) and at Macrogen (MD, USA). PCR amplification and bidirectional sequencing were performed at least twice from 2 independently DNA-extracted tissue samples. Contigs were assembled by combining corresponding forward and reverse sequences, and the consensus sequence was aligned using the Clustal W accessory application in BioEdit 1.0.9.0 (Hall 1999). A BLAST search was completed to determine similarity with other sequences in GenBank. Sequences with >80% sequence similarity and >98% query coverage were included in the alignment along with representatives of each of the 5 major microsporidian groups and 3 non-microsporidian outgroup organisms (as per Vossbrinck & Debrunner-Vossbrinck 2005) to determine the identity and phylogenetic placement within the microsporidia. This preliminary phylogenetic analysis of 76 sequences (data not shown) indicated that the *Caretta caretta* microsporidian sequence (GenBank accession number MF373108) belongs to the Marinosporidia (Clade III sensu Vossbrinck & Debrunner-Vossbrinck 2005). The refined alignment and phylogeny of 44 sequences included the *C. caretta* microsporidian sequence with related Marinosporidia ingroups and single representatives of each microsporidian clade and the 3 outgroup organisms. Phylogenies were constructed by neighbour-joining (NJ), maximum parsimony (MP) and maximum likelihood (ML) methods using MEGA version 6.0 (Tamura et al. 2013). Statistical support for NJ, ML and MP tree topologies were bootstrap sampled 1000 times, and support values (%) of NJ, MP and ML analysis were superimposed on the NJ consensus trees.

For phylogeny reconstruction, NJ tree evolutionary distances were computed using the Tamura-Nei method (Tamura & Nei 1993) and are in the units of the number of base substitutions per site. The rate variation among sites was modeled with a gamma distribution (shape parameter = 1). The MP tree was obtained using the subtree pruning–regrafting algorithm (Nei & Kumar 2000) with search level 1, in which the initial trees were obtained with the random addition of sequences (10 replicates). The ML tree was constructed using the general time reversible model + G substitution model (Nei & Kumar 2000) as determined by the lowest Bayesian information criterion score and highest corrected Akaike's information criterion value (Tamura et al. 2013). Initial trees for the heuristic search were obtained automatically by applying NJ and BioNJ algorithms to a matrix of pairwise distances estimated using the maximum composite likelihood approach and then selecting the topology with superior log likelihood value. A discrete Gamma distribution was used to model evolutionary rate differences among sites, 5 categories + G, parameter = 0.9224. The final dataset contained 44 nucleotide sequences using 1038 positions. All positions containing gaps and missing data were eliminated. Bootstrap values (1000 replicates) for each NJ, MP and ML tree were computed following Felsenstein (1985).

RESULTS

Histopathology

Significant changes were identified within the skeletal muscle and the alimentary tract. Sections of skeletal muscle were examined from all 4 limbs, the pectoral girdle and the epaxial region (15 muscle samples in total). In all sections, there was multifocal infiltration of the skeletal muscle by inflammatory cells consisting primarily of macrophages with fewer

lymphocytes and plasma cells. These cells infiltrated the perimysium, often invading and replacing myofibers. In the affected areas, there were scattered swollen, occasionally fragmented hypereosinophilic myofibers lacking striations (degeneration and necrosis) (Fig. 1). Numerous small (1.1–1.7 × 2.2–3.4 µm) ovoid spores were present free among the inflammatory infiltrates (Fig. 2). These organisms had a densely basophilic round central structure surrounded by a clear, slightly refractile wall. Similar spores were often clustered in groups of 12 to 22 and invested within a thick-walled sporophorous vesicle (Fig. 2). Away from the areas of inflammation were rare myofibers containing large (approximately 300 × 70 µm) sporophorocysts consisting of numerous densely clustered sporophorous vesicles (Fig. 3). Special stains (Gram, PAS and ZN acid-fast) were applied to the sections. The spores stained weakly Gram positive, had weak punctate positive PAS reaction and were occasionally strongly acid fast (Fig. 2). Small linear birefringent structures were present in the spores when viewed under polarized light. The histologic diagnosis was subacute histiocytic myositis with myofiber necrosis and intralesional microsporidia.

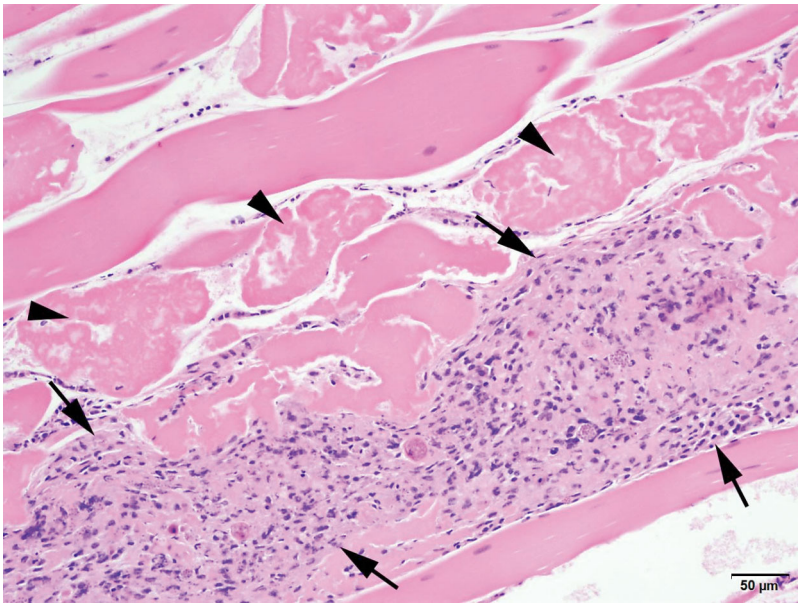

Fig. 1. Skeletal muscle from *Caretta caretta* with a band-like inflammatory infiltrate (arrows) and myofiber degeneration and necrosis with flocculent change in the cytoplasm (arrowheads) (H&E)

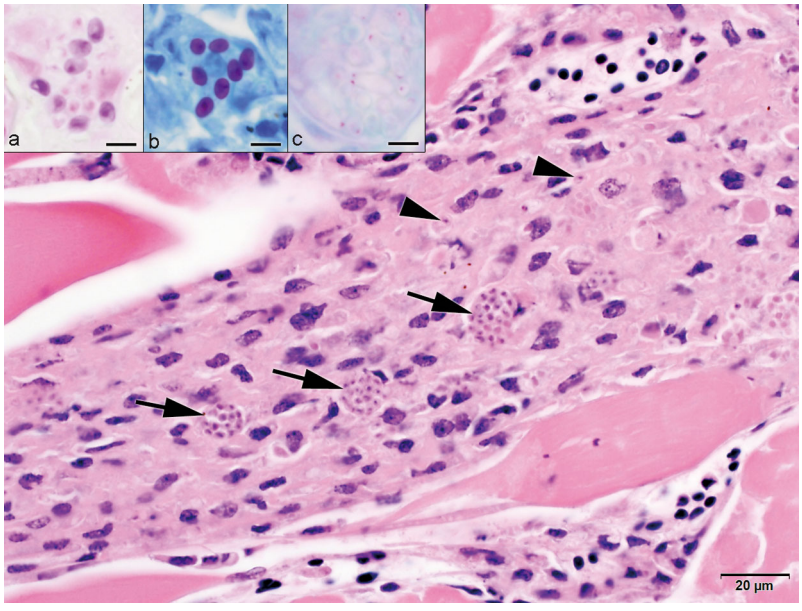

Fig. 2. Skeletal muscle from *Caretta caretta* with inflammation and intralesional microsporidial spores scattered freely (arrowheads) among the infiltrates or present within sporophorous vesicles (arrows) (hematoxylin and eosin). Insets: spores (a) are weakly Gram positive (Gram stain), (b) occasionally have strong acid-fast staining (ZN acid-fast stain) and (c) show punctate PAS-positive reaction. Scale bar 4 µm

In the stomach and small intestine, there was multifocal erosion and infiltration of the superficial mucosa by small to moderate numbers of heterophils with fibrin covering the denuded mucosa. A fibrin cast in the small intestinal lumen was embedded with degenerate heterophils, erythrocytes, a few cross sections of trematodes (not further identified), and scattered colonies of mixed Gram-positive and Gram-negative bacteria. No microsporidia were observed. Present within the gastric submucosa were rare cross sections of nematodes (not further identified) surrounded by a rim of eosinophilic debris and mild granulomatous inflammation. Histologic diagnoses for the gastrointestinal tract were acute segmental heterophilic and fibrinous gastroenteritis and mild chronic gastric submucosal parasitic granulomas. Minimal lymphoplasmacytic infiltrates were present in the kidney and the

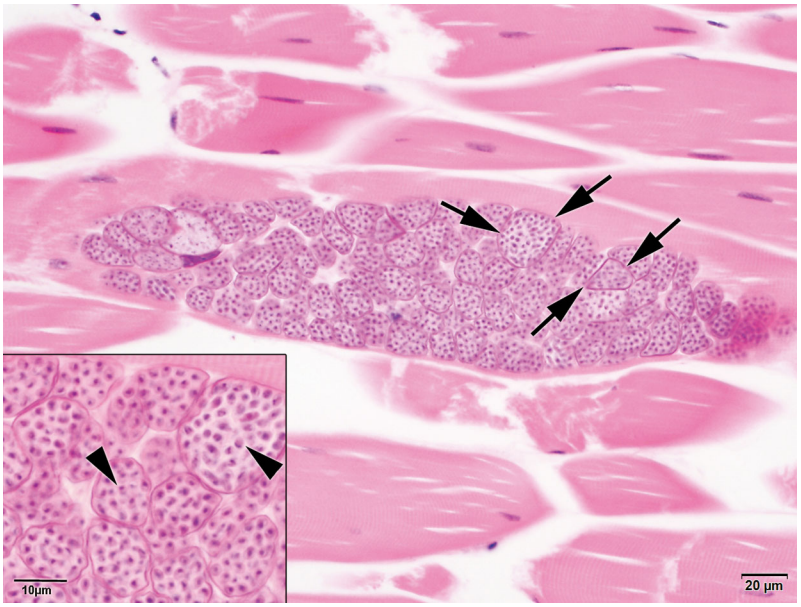

Fig. 3. Skeletal muscle from *Caretta caretta* containing a large sporophorocyst composed of multiple sporophorous vesicles (delineated by arrows). Inset: microsporidial spores (arrowheads) within the sporophorous vesicles (H&E)

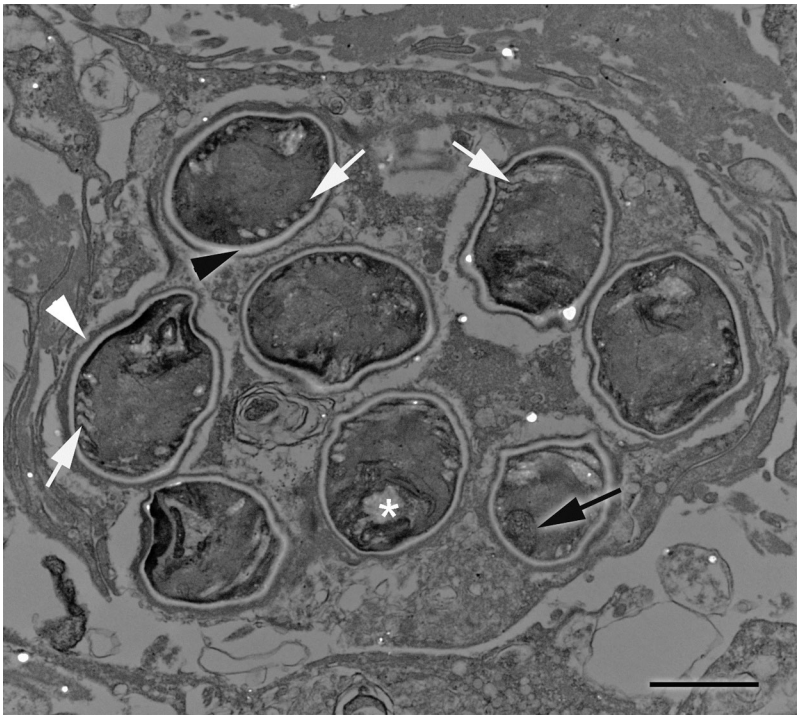

Fig. 4. Transmission electron micrograph of the skeletal muscle from *Caretta caretta* containing microsporidial spores within a sporophorous vesicle. Ultrastructural features of the spores include an electron-dense exospore (white arrowhead), an electron-lucent endospore (black arrowhead), a coiled polar filament (white arrows), a single nucleus (black arrow) and a posterior vacuole (asterisk). Scale bar 2 µm

pulmonary interstitium, and the remaining organs were unremarkable.

Transmission electron microscopy

Postmortem autolysis and freeze–thaw artefacts were moderate in areas. Evaluation was restricted to the best-preserved regions. Identified within the skeletal muscle were several 1.5–2.0 × 2.5–3.0 µm microsporidial spores present individually and in aggregates of 8 to 13 within sporophorous vesicles. The spores had a thick wall consisting of an electron-dense exospore, an inner electron-lucent endospore and the innermost plasma membrane (Fig. 4). Each had a single eccentric nucleus, a posterior vacuole and a coiled polar filament. The number of paired coils in the polar filament was difficult to discern, with 7 to 10 coils counted in most spores.

SSU rRNA gene sequence and phylogeny

The phylogenetic analysis of SSU rRNA partial gene sequences from 44 microsporidians was assessed by NJ, MP and ML analysis (Fig. 5). The *Caretta caretta* microsporidian sequence (MF373108, which was identified in both skeletal muscle and small intestine) shares 98.2 to 99.8% similarity with the members of an ingroup that includes *Microsporidium prosopium* (AF151529.1), *Microsporidia spraguei* (KU302781.1, KX351970.1), *Myosporidium merluccius* (AY530532.1), *Heterosporis* sp. (KC137554.1) and Microsporidia sp. (KU302784.1, KU302789.1), which was well supported by high (100%) bootstrap values (Table 1, Fig. 5). The *C. caretta* microsporidian sequence forms a sister-group association with *Microsporidium prosopium* supported by moderate to high bootstrap values of 70, 96 and 65% by the NJ, MP and ML methods, respectively (Fig. 5).

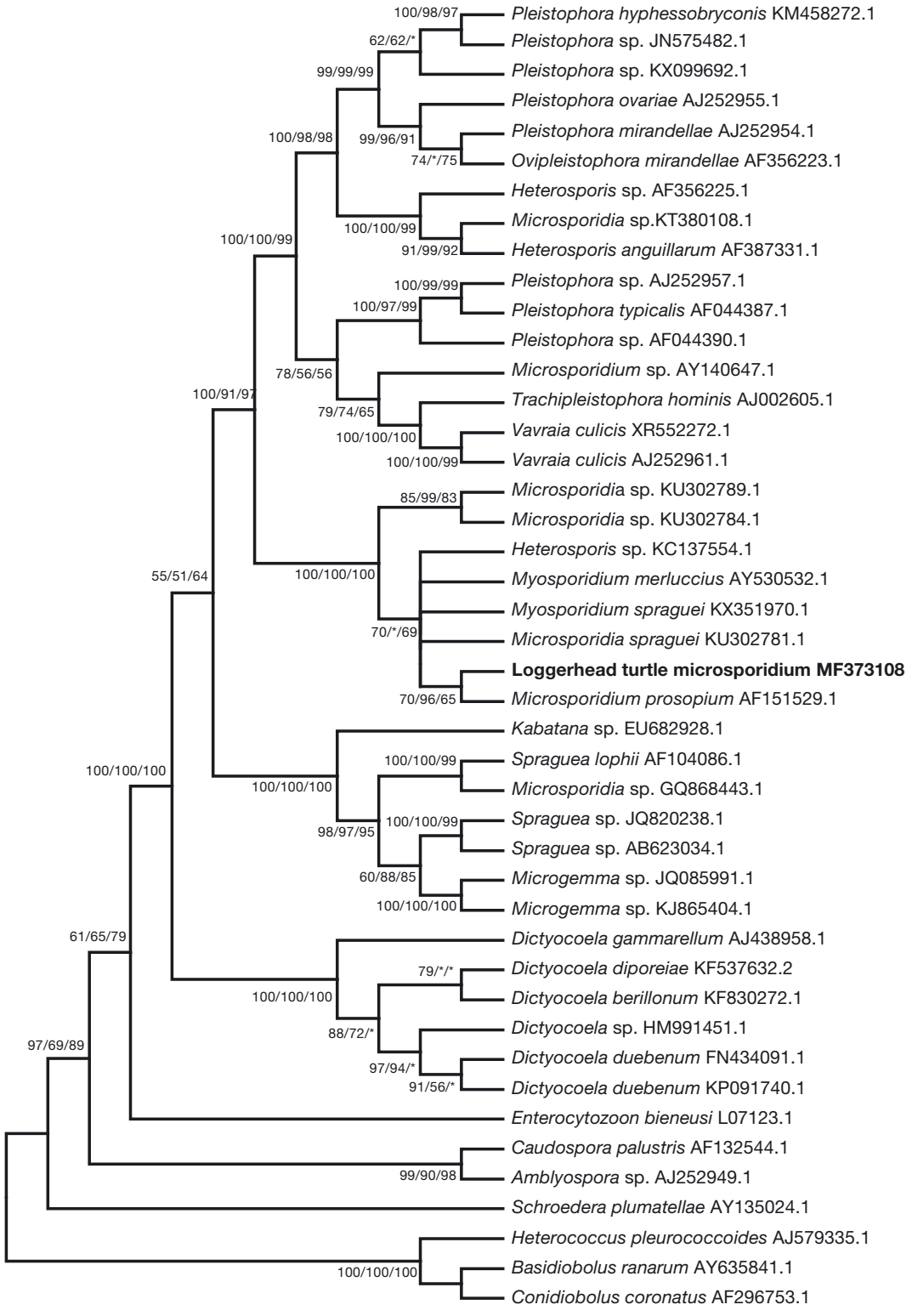

Fig. 5. Neighbour-joining 50% bootstrap-consensus tree based on microsporidium small subunit rRNA gene sequences. Values at nodes represent the bootstrap percentages from 1000 replicates for neighbor joining, maximum parsimony and maximum likelihood, respectively. The final dataset contained 44 sequences and 1038 positions, as all positions containing gaps and missing data were eliminated. Sequences are indicated by the organism name followed by the GenBank accession number. The newly described loggerhead sea turtle *Caretta caretta* microsporidian sequence is in **bold**

Table 1. Percent identities of the small subunit rRNA gene from a *Caretta caretta* microsporidium (MF373108) compared to an ingroup of previously reported microsporidians. Based on alignment of 1280 nucleotide positions

	Microsporidian name	1	2	3	4	5	6	7	8
1	Loggerhead turtle microsporidium MF373108								
2	*Heterosporis* sp. KC137554.1	0.998							
3	*Microsporidium prosopium* AF151529.1	0.992	0.992						
4	*Myosporidium merluccius* AY530532.1	0.995	0.996	0.989					
5	*Myosporidium spraguei* KX351970.1	0.992	0.994	0.987	0.992				
6	Microsporidia sp. KU302781.1	0.992	0.994	0.987	0.992	1			
7	Microsporidia sp. KU302789.1	0.982	0.984	0.977	0.982	0.980	0.980		
8	Microsporidia sp. KU302784.1	0.989	0.990	0.983	0.989	0.986	0.986	0.993	

DISCUSSION

Microsporidia have been classified according to morphologic features such as nuclear number, number of coils in the polar filament, and formation of sporophorous vesicles or xenomas as identified using electron and light microscopy (Narasimhamurti et al. 1982, Eydner et al. 2017). While microscopy can be diagnostic for microsporidial infection, the morphology of these organisms is plastic and can change rapidly within a genus and species (Stentiford et al. 2013a), favouring the use of molecular techniques for speciation of these organisms (Vossbrinck & Debrunner-Vossbrinck 2005, Ghosh & Weiss 2009). The most common diagnostic test used is PCR for the SSU rRNA gene followed by DNA sequencing (Vossbrinck et al. 2004, Vossbrinck & Debrunner-Vossbrinck 2005, Ghosh & Weiss 2009).

Using phylogenetic analysis based on the SSU rRNA gene sequence, microsporidia have been classified into 3 major classes based on habitat and host species affected, with further subdivision into 5 clades (Vossbrinck & Debrunner-Vossbrinck 2005). The classes are Aquasporidia, which includes 3 clades that infect primarily freshwater hosts; Marinosporidia, with 1 clade infecting primarily marine hosts; and Terresporidia, with 1 clade infecting primarily terrestrial hosts (Vossbrinck & Debrunner-Vossbrinck 2005). The microsporidium detected in this loggerhead sea turtle appears to represent a new species within the class Marinosporidia and clusters closely with *Microsporidium prosopium, Microsporidia spraguei*, *Myosporidium merluccius*, *Heterosporis* sp. and *Microsporidia* sp.

Microsporidia are typically considered opportunistic pathogens and may be shed in the feces of healthy reptiles (Graczyk & Cranfield 2000). Significant infections tend to occur in animals with concurrent viral and parasitic infections (Jacobson et al. 1998) but have also been reported in reptiles with no obvious predisposing conditions, suggesting that microsporidia may act as primary pathogens (Scheelings et al. 2015). The reptile species most frequently affected by microsporidiosis is the inland bearded dragon *Pogona vitticeps*. These captive lizards develop systemic granulomas and necrosis in association with an *Encephalitozoon* sp. infection (Jacobson et al. 1998, Mitchell & Garner 2011, Richter et al. 2013); this pathogen has recently been named *Encephalitozoon pogonae* (Sokolova et al. 2016).

Other species of microsporidia that infect reptiles include *Heterosporis anguillarum*, which was associated with localized myositis in the garter snake *Thamnophis sirtalis* (Richter et al. 2014); a *Heterosporis*-like microsporidian, causing myositis in Australian sea snakes *Hydrophis* spp. (Gillett et al. 2016); *Encephalitozoon hellem*, causing hepatitis in freshwater crocodiles *Crocodylus johnstoni* (Scheelings et al. 2015); *Pleistophora atretii*, causing myositis in freshwater snakes *Atretium schistosum* Günther (Narasimhamurti et al. 1982); *Encephalitozoon cuniculi*, infecting the intestine of pink-tongued skinks *Hemisphaeriodon gerrardi* (Garner et al. 2000); *Encephalitozoon* (not further speciated), causing enteritis in African skinks *Mabuya perrotetii* (Koudela et al. 1998); and *Pleistophora* (not further speciated), causing myositis in a captive tuatara (Liu & King 1971).

Until recently, microsporidiosis had not been reported in turtles or tortoises. Microsporidiosis was diagnosed in 4 captive Hermann's tortoises *Testudo hermanni boettgeri* with enteritis, hepatitis and pneumonia. The intralesional microsporidial spores were identified as *Encephalitozoon* sp. based on spore morphology (Eydner et al. 2017). These infections all occurred when the tortoises emerged from hibernation, and it was speculated that immunosuppression played a predisposing role (Eydner et al. 2017). It has been suggested that the common theme underlying the apparent emergence of these patho-

gens in multiple different species from varying environments, or biomes, is altered immunocompetence of host species (Stentiford et al. 2016).

In this loggerhead sea turtle, microsporidia were present in large numbers in multiple muscles, and considerable necrosis and inflammation were associated with this infection. Muscle infection and myositis are seemingly common in reptiles with microsporidiosis (Liu & King 1971, Narasimhamurti et al. 1982, Richter et al. 2014, Gillett et al. 2016), and these lesions may contribute to morbidity via muscular pain and weakness, which impede normal swimming and feeding behaviour and increase the likelihood of traumatic injury and stranding (Gillett et al. 2016). Concurrent gastroenteritis was detected and was deemed significant in this sea turtle. Microsporidia were not visible within the gastrointestinal lesion using microscopy; however, these organisms can be difficult to detect in histologic section. The small intestinal tissue tested positive for microsporidia using PCR and shared sequence identity with the organism identified in the muscle. Scant growth of *Serratia liquefaciens* was isolated from affected intestine; however, both Gram-positive and Gram-negative bacteria were evident in the histologic sections, as were small numbers of trematodes. Gastroenteritis likely occurred as a result of mixed bacterial, microsporidial and trematode infection in this sea turtle. Microsporidial infection of the enterocytes in the intestine may lead to enteritis in reptiles and supports the possibility of fecal–oral transmission for these organisms (Koudela et al. 1998, Garner et al. 2000, Richter et al. 2013). The presence of multiple opportunistic invaders may suggest underlying immunosuppression. Given the timing of death in the late fall, it is possible that cold-stunning (hypothermia) led to immunosuppression (Hunt et al. 2012), predisposing to or exacerbating these disease processes and hastening death.

In summary, a novel microsporidial species caused significant myositis and likely contributed to gastroenteritis in a juvenile female loggerhead sea turtle from the Northwest Atlantic DPS and likely contributed to the mortality of this animal. This case is the first report of microsporidiosis in a sea turtle and adds to the limited literature regarding infectious diseases in these vulnerable species. In the future, thorough histologic evaluation of the musculature of these animals during postmortem examination is warranted to gauge the importance and prevalence of microsporidial infections in sea turtles.

Acknowledgements. The authors thank Haili Wang for technical support. The diagnostic work was done as part of the wildlife health surveillance program of the Canadian Wildlife Health Cooperative.

LITERATURE CITED

Bolten AB, Crowder LB, Dodd MG, MacPherson SL and others (2011) Quantifying multiple threats to endangered species: an example from loggerhead sea turtles. Front Ecol Environ 9:295–301

Casale P, Tucker AD (2015) *Caretta caretta*. The IUCN Red List of Threatened Species: e.T3897A83157651. http://dx.doi.org/10.2305/IUCN.UK.2015-4.RLTS.T3897A83157651.en (accessed on 9 Aug 2017)

DFO (Department of Fisheries and Oceans Canada) (2017) Threat assessment for loggerhead sea turtle (*Caretta caretta*), Northwest Atlantic population. DFO Can Sci Advis Sec Sci Resp 2017/014

Eydner M, Donhauser J, Beineke A, Guenther P, Blahak S (2017) Microsporidiosis in four tortoises (*Testudo hermanni boettgeri*). Vet Pathol 54:704–709

Felsenstein J (1985) Confidence limits on phylogenies: an approach using the bootstrap. Evolution 39:783–791

Galois P, Ouelett M (2007) Health and disease in Canadian reptile populations. In: Seburn CNL, Bishop CA (eds) Ecology, conservation and status of reptiles in Canada. Society for the Study of Amphibians and Reptiles, Salt Lake City, UT

Garner M, Collins D, Joslin J, Didler E, Nordhausen R (2000) Microsporidiosis in a closed colony of pink-tongued skinks, *Hemisphaeriodon gerrardi*. In: Proc 7th Ann Conf Assoc Reptilian Amphib Veterinarians, 18–22 October 2000, Reno, NV. Association of Reptilian and Amphibian Veterinarians, Gainesville, FL, p 57–58

Ghosh K, Weiss LM (2009) Molecular diagnostic tests for microsporidia. Interdiscip Perspect Infect Dis 2009: 926521

Gillett AK, Ploeg R, O'Donoghue PJ, Chapman PA, Webb RI, Flint M, Mills PC (2016) Ultrastructural and molecular characterisation of an *Heterosporis*-like microsporidian in Australian sea snakes (Hydrophiinae). PLOS ONE 11: e0150724

Graczyk TK, Cranfield MR (2000) *Cryptosporidium serpentis* oocysts and microsporidian spores in feces of captive snakes. J Parasitol 86:413–414

Hall TA (1999) BioEdit: a user friendly biological sequence alignment editor and analysis program for Windows 95/98/NT. Nucleic Acids Symp Ser 41:95–98

Hunt KE, Innis C, Rolland RM (2012) Corticosterone and thyroxine in cold-stunned Kemp's ridley sea turtles (*Lepidochelys kempii*). J Zoo Wildl Med 43:479–493

Jacobson ER, Green DE, Undeen AH, Cranfield M, Vaughn KL (1998) Systemic microsporidiosis in inland bearded dragons (*Pogona vitticeps*). J Zoo Wildl Med 29:315–323

James TY, Pelin A, Bonen L, Ahrendt S, Sain D, Corradi N, Stajich JE (2013) Shared signatures of parasitism and phylogenomics unite Cryptomycota and microsporidia. Curr Biol 23:1548–1553

Koudela B, Didier ES, Rogers LB, Modry D, Kucerova S (1998) Intestinal microsporidiosis in African skink, *Mabuya perrotetii*. Folia Parasitol 45:149–155

Liu SK, King FW (1971) Microsporidiosis in the tuatara. J Am Vet Med Assoc 159:1578–1582

Mitchell M, Garner M (2011) Microsporidiosis in bearded dragons: a case for vertical transmission. In: Proc 18th Ann Conf Assoc Reptilian Amphib Veterinarians, 7–12 August, Seattle, WA. Association of Reptilian and Amphibian Veterinarians, Gainesville, FL, p 123

Narasimhamurti CC, Kalavati C, Ahamed SN (1982) A new microsporidian, *Pleistophora atretii* sp. n. from the fresh water snake, *Atretium schistosum* Günther. Acta Protozool 21:127–137

Nei M, Kumar S (2000) Molecular evolution and phylogenetics. Oxford University Press, New York, NY

Richter B, Csokai J, Graner I, Eisenberg T, Pantchev N, Eskens HU, Nedorost N (2013) Encephalitozoonosis in two inland bearded dragons (*Pogona vitticeps*). J Comp Pathol 148:278–282

Richter B, Graner I, Csokai J (2014) *Heterosporis anguillarum* infection in a garter snake (*Thamnophis sirtalis*). J Comp Pathol 150:332–335

Scheelings TF, Slocombe RF, Crameri S, Hair S (2015) *Encephalitozoon hellem* infection in a captive juvenile freshwater crocodile (*Crocodylus johnstoni*). J Comp Pathol 153:352–356

Sokolova YY, Sakaguchi K, Paulsen DB (2016) Establishing a new species *Encephalitozoon pogonae* for the microsporidian parasite of inland bearded dragon *Pogona vitticeps* Ahl 1927 (Reptilia, Squamata, Agamidae). J Eukaryot Microbiol 63:524–535

Stentiford GD, Bateman KS, Feist SW, Chambers E, Stone DM (2013a) Plastic parasites: extreme dimorphism creates a taxonomic conundrum in the phylum Microsporidia. Int J Parasitol 43:339–352

Stentiford GD, Feist SW, Chambers E, Stone DM, Bateman KS, Dunn AM (2013b) Microsporidia: diverse, dynamic and emergent pathogens in aquatic systems. Trends Parasitol 29:567–578

Stentiford GD, Becnel JJ, Weiss LM, Keeling PJ and others (2016) Microsporidia — emergent pathogens in the global food chain. Trends Parasitol 32: 336–348

Tamura K, Nei M (1993) Estimation of the number of nucleotide substitutions in the control region of mitochondrial DNA in humans and chimpanzees. Mol Biol Evol 10: 512–526

Tamura K, Stecher G, Peterson D, Filipski A, Kumar S (2013) MEGA6: molecular evolutionary genetics analysis version 6.0. Mol Biol Evol 30:2725–2729

Vossbrinck CR, Debrunner-Vossbrinck BA (2005) Molecular phylogeny of the microsporidia: ecological, ultrastructural and taxonomic considerations. Folia Parasitol 52: 131–142

Vossbrinck CR, Andreadis TG, Vavra J, Becnel JJ (2004) Molecular phylogeny and evolution of mosquito parasitic microsporidia (Microsporidia: Amblyosporidae). J Eukaryot Microbiol 51:88–95

Editorial responsibility: Thierry Work, Honolulu, Hawaii, USA

Submitted: November 3, 2017; Accepted: April 10, 2018
Proofs received from author(s): May 30, 2018